

# Supporting Information

## ***In situ Raman Evidence of Intermediates Adsorption Engineering by High-Index Facets Control during Hydrogen Evolution Reaction***

Jia-sen Zhu,<sup>†a</sup> Hao Yang,<sup>†b</sup> Weihong Zhang,<sup>b</sup> Yanchao Mao,<sup>\*c</sup> Shu-shen Lyu,<sup>\*d</sup> and Jian Chen<sup>\*c</sup>

<sup>a</sup>School of Chemical Engineering and Technology, Sun Yat-sen University, Zhuhai 519082, China

<sup>b</sup>School of Materials Science and Engineering, Instrumental analysis and Research center, Sun Yat-sen University, Guangzhou 510275, China

<sup>c</sup>MOE Key Laboratory of Materials Physics, School of Physics and Microelectronics, Zhengzhou University, Zhengzhou 450001, China

<sup>d</sup>School of Materials, Sun Yat-sen University, Guangzhou 510006, China

**Keywords:** *In-situ Raman, Intermediates adsorption, Hydrogen evolution reaction, TiO<sub>2</sub> nanosheets*

### **List of contents**

Figure S1. SEM images of clean Ti mesh and Ti@TiO <sub>2</sub> nanosheets under different hydrothermal time. ....	3
Figure S2. TEM images of Ti@TiO <sub>2</sub> -6H nanosheets under different hydrothermal time. ....	4
Figure S3. TEM images of Ti@TiO <sub>2</sub> -3H nanosheets. ....	4
Figure S4. XRD patterns and Raman spectra of Ti@TiO <sub>2</sub> nanosheets under different hydrothermal time. ....	5
Figure S5. Core-level XPS spectra of Ti@TiO <sub>2</sub> nanosheets under different hydrothermal time. ....	5
Figure S6. Tafel plots and electrochemical impedance spectra of Ti@TiO <sub>2</sub> nanosheets under different hydrothermal time. ....	5

Figure S7. The electrochemical active surface areas of Ti mesh and Ti@TiO <sub>2</sub> nanosheets under different hydrothermal time .....	6
Figure S8. The contact angles of a drop of 1.0 M KOH on Ti mesh and Ti@TiO <sub>2</sub> nanosheets under different hydrothermal time. ....	7
Figure S9. Electron density difference collected for H <sub>2</sub> O adsorption, surface atoms of (a) TiO <sub>2</sub> (301) and (b) TiO <sub>2</sub> (303). ....	7
Figure S10. In situ Raman spectra of Ti@TiO <sub>2</sub> -3H nanosheets in a 1.0 M KOH solution. ....	7
Figure S11. In situ Raman spectra of Ti@TiO <sub>2</sub> -6H nanosheets in a 1.0 M KOH solution. ....	8
Figure S12. In situ Raman spectra of Ti@TiO <sub>2</sub> -12H nanosheets in a 1.0 M KOH solution. ....	8
Figure S13. In situ Raman spectra of Ti@TiO <sub>2</sub> -18H nanosheets in a 1.0 M KOH solution. ....	8
Figure S14. In situ Raman spectra of Ti@TiO <sub>2</sub> -24H nanosheets in a 1.0 M KOH solution. ....	8
Figure S15. In situ Raman spectra of H adsorption on the Ti@TiO <sub>2</sub> -6H nanosheets in a 1.0 M KOH solution. ....	9
Figure S16. In situ Raman spectra of anatase Ti@TiO <sub>2</sub> -6H nanosheets in 1.0 M KOH or 1.0 M KOD solution below 1200 cm <sup>-1</sup> . ....	9
Figure S17. Time-resolved Raman spectra of Ti@TiO <sub>2</sub> -6H nanosheets from 0 V to -0.5 V vs. RHE in a solution 0.5 M KOH. ....	10
Figure S18. (a) The three peaks of interfacial water at ~3500 cm <sup>-1</sup> of Ti@TiO <sub>2</sub> -6H nanosheets from 0 V to -0.5 V vs. RHE in different solution: (a) 0.5 M KOH + 0.5 M KOD and (b) 1 M KOH. ....	10
Figure S19. The normalized intensity of the three peaks of interfacial water on the surface of Ti@TiO <sub>2</sub> nanosheets with different hydrothermal time at -0.5 V vs. RHE in 1.0 M KOH solution. ....	10
Figure S20. (a) Synchronous and (b) asynchronous 2D correlation Raman spectra of the interfacial water on the surface of Ti@TiO <sub>2</sub> -6H nanosheets from 0 V to -0.6 V vs. RHE. ....	11

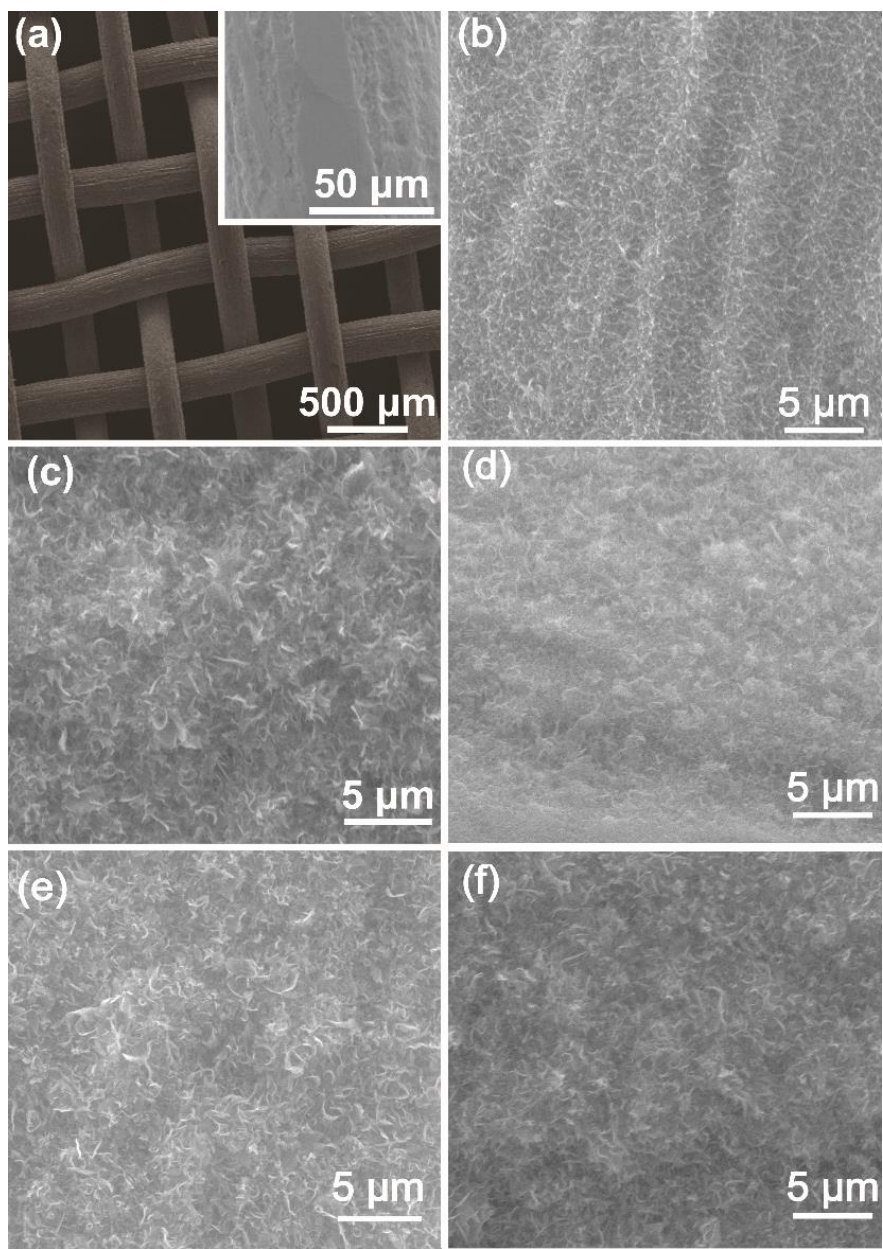


Figure S1. SEM images of (a) clean Ti mesh and Ti@TiO<sub>2</sub> nanosheets under different hydrothermal time: (b) 3 h, (c) 6 h, (d) 12 h (e) 18h and (d) 24 h.

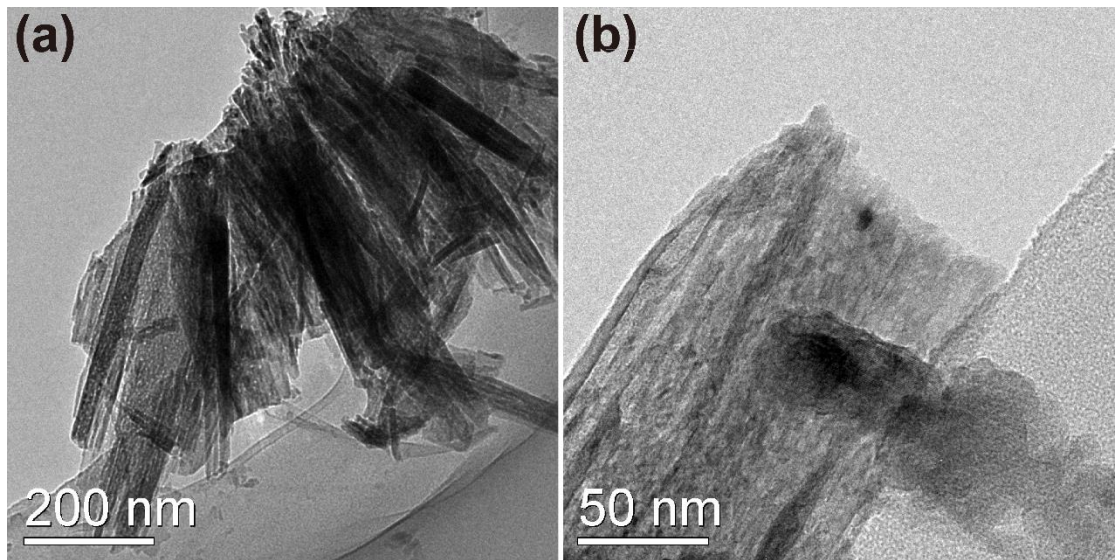


Figure S2. TEM images of Ti@TiO<sub>2</sub>-6H nanosheets under different hydrothermal time.

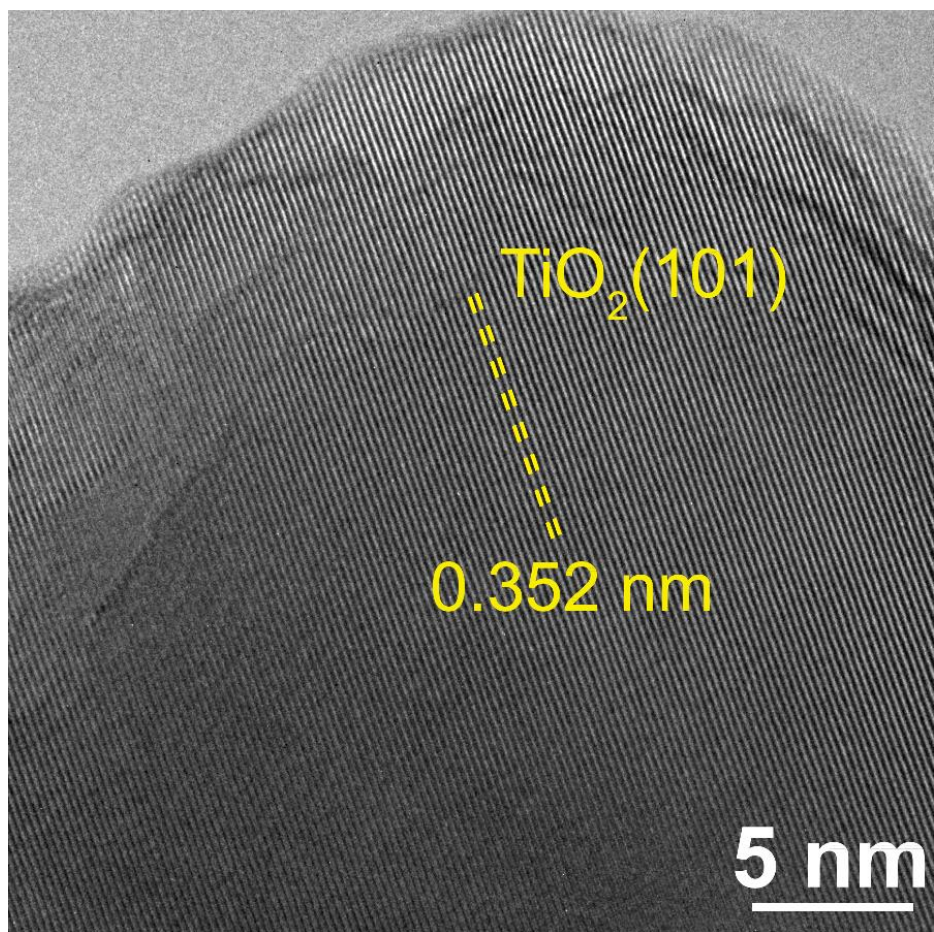


Figure S3. TEM images of Ti@TiO<sub>2</sub>-3H nanosheets.

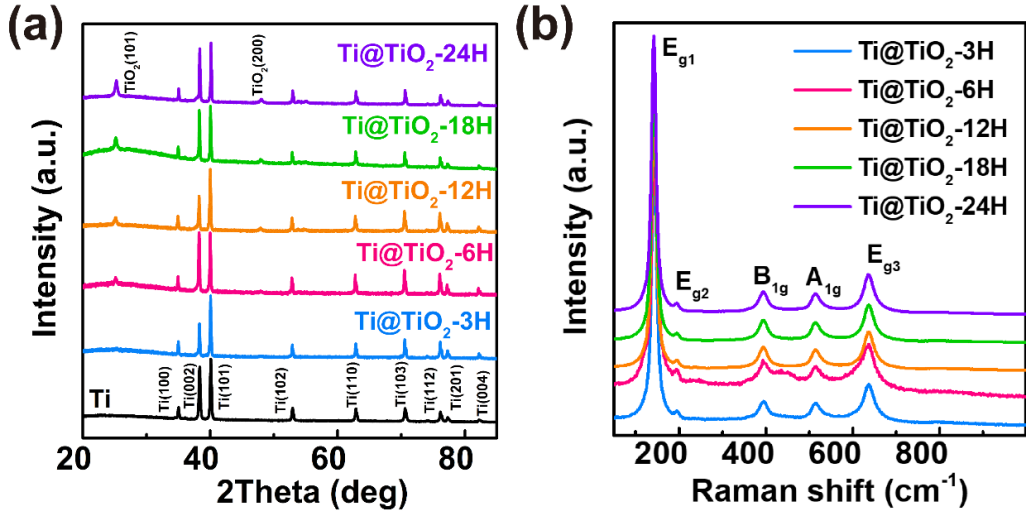


Figure S4. (a) XRD patterns and (b) Raman spectra of Ti@TiO<sub>2</sub> nanosheets under different hydrothermal time.

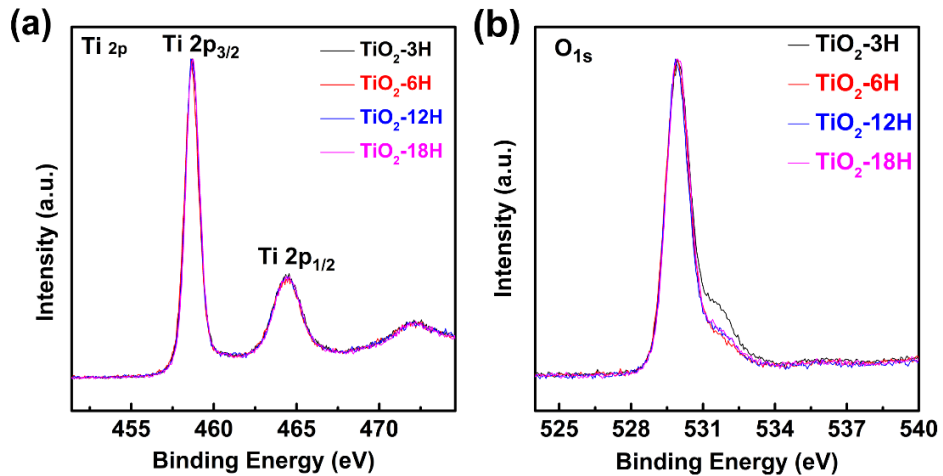


Figure S5. Core-level (a) Ti 2p and (b) O 1s XPS spectra of Ti@TiO<sub>2</sub> nanosheets under different hydrothermal time.

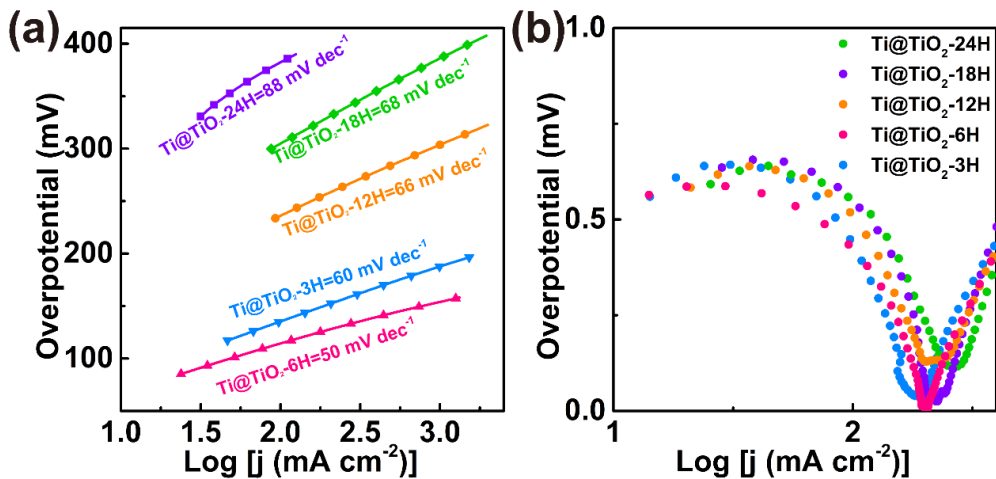


Figure S6. (a) Tafel plots and (b) electrochemical impedance spectra of Ti@TiO<sub>2</sub> nanosheets under different hydrothermal time.

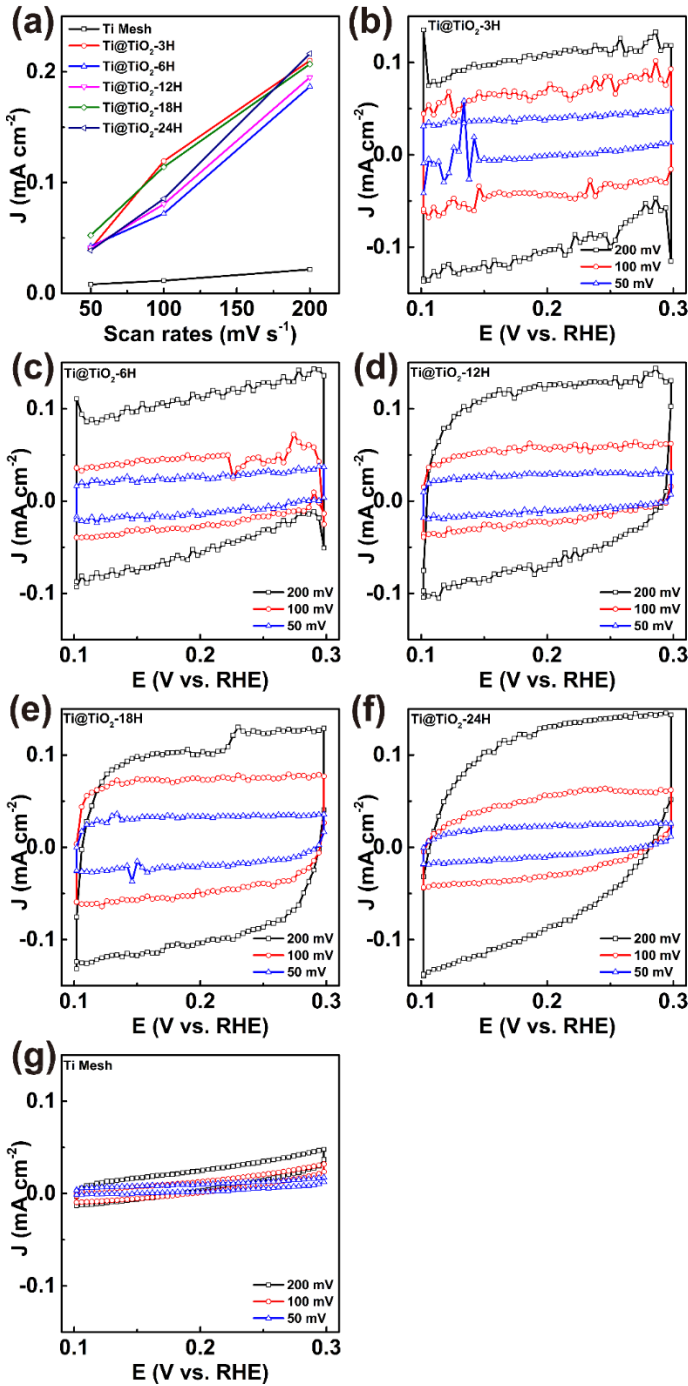


Figure S7. (a) The electrochemical active surface areas of Ti mesh and  $\text{Ti@TiO}_2$  nanosheets under different hydrothermal time were determined by the capacitance of the double layer ( $C_{dl}$ ) from the cyclic voltammetry (CV) curves of the catalysts between 0.1 and 0.3 V (V vs. RHE): (b)  $\text{Ti@TiO}_2$ -3H nanosheets, (c)  $\text{Ti@TiO}_2$ -6H nanosheets, (d)  $\text{Ti@TiO}_2$ -12H nanosheets, (e)  $\text{Ti@TiO}_2$ -18H nanosheets, (f)  $\text{Ti@TiO}_2$ -24H nanosheets and (g) Ti mesh. The slope of different sample in Figure S7a is proportional to the electrochemical active surface area.

The electrochemical active surface areas of  $\text{Ti@TiO}_2$  nanosheets were determined by the capacitance of the double layer ( $C_{dl}$ ) from the cyclic voltammetry (CV) curves of the catalysts. The slope of different samples in Figure S7a is proportional to the electrochemical active surface area. It is worth noting that the electrochemical active surface areas of  $\text{Ti@TiO}_2$  nanosheets under different hydrothermal time are almost the same.

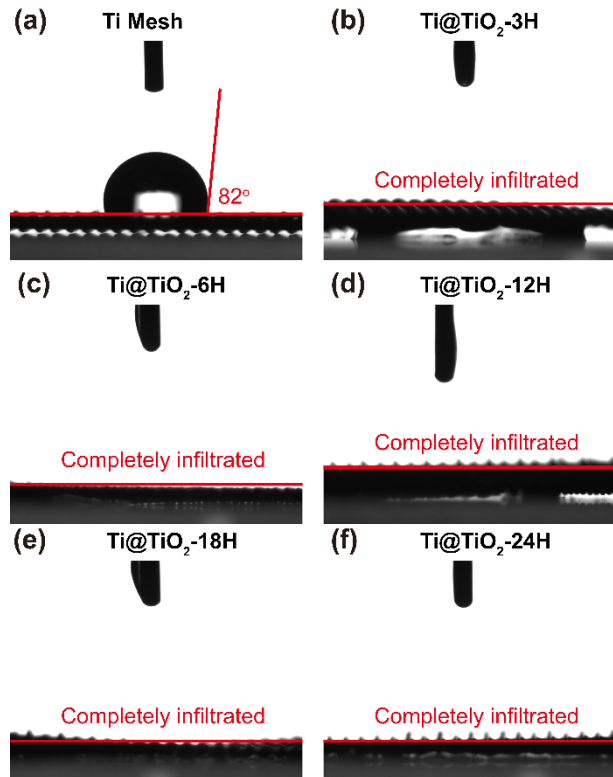


Figure S8. The contact angles of a drop of 1.0 M KOH on (a) Ti mesh and Ti@TiO<sub>2</sub> nanosheets under different hydrothermal time: (b) 3 h, (c) 6 h, (d) 12 h (e) 18h and (d) 24 h.

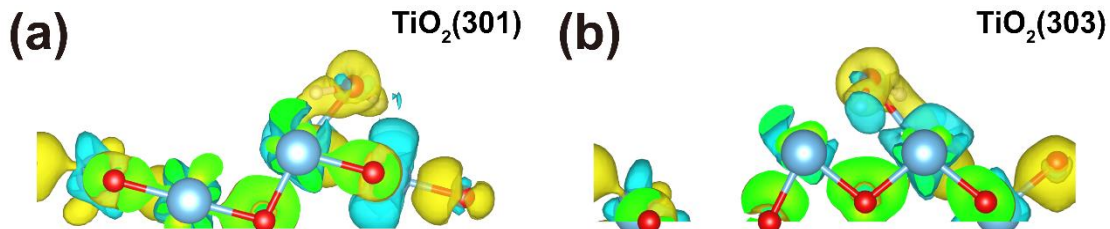


Figure S9. Electron density difference collected for H<sub>2</sub>O adsorption, surface atoms of (a) TiO<sub>2</sub>(301) and (b) TiO<sub>2</sub>(303). Blue and red refer to the charge depletion and charge accumulation, respectively. Light blue, Ti atoms; Red, O atoms; Pink, H atoms.

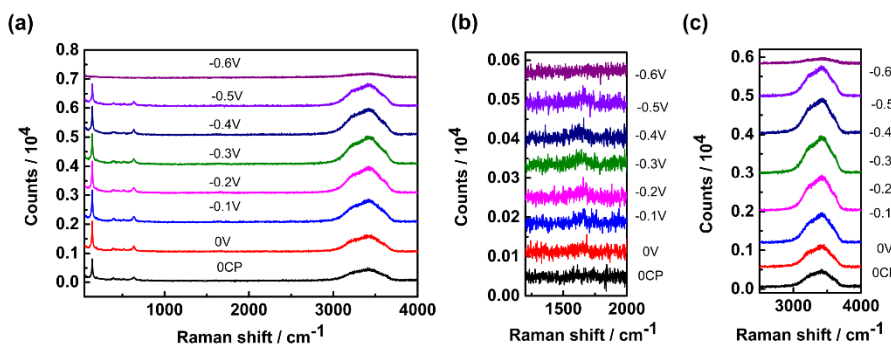


Figure S10. In situ Raman spectra of Ti@TiO<sub>2</sub>-3H nanosheets in a 1.0 M KOH solution.

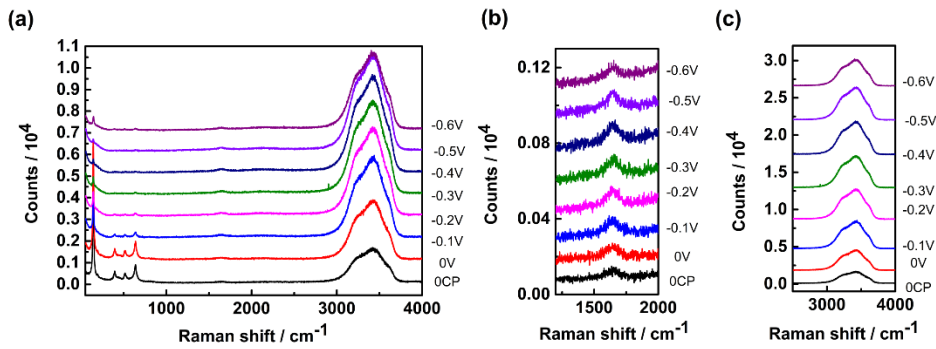


Figure S11. In situ Raman spectra of Ti@TiO<sub>2</sub>-6H nanosheets in a 1.0 M KOH solution.

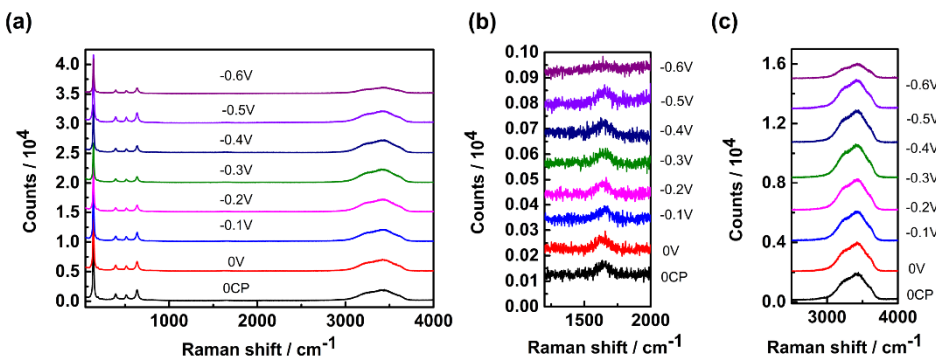


Figure S12. In situ Raman spectra of Ti@TiO<sub>2</sub>-12H nanosheets in a 1.0 M KOH solution.

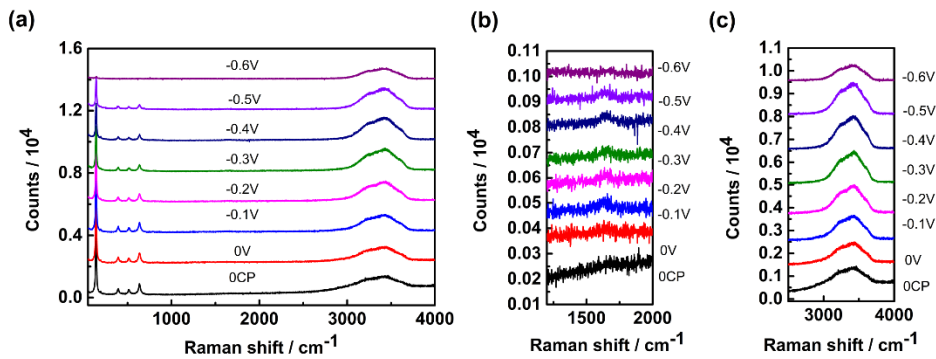


Figure S13. In situ Raman spectra of Ti@TiO<sub>2</sub>-18H nanosheets in a 1.0 M KOH solution.

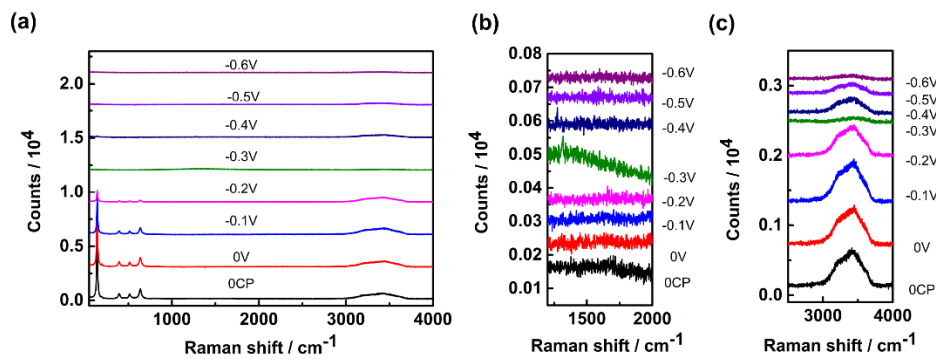


Figure S14. In situ Raman spectra of Ti@TiO<sub>2</sub>-24H nanosheets in a 1.0 M KOH solution.

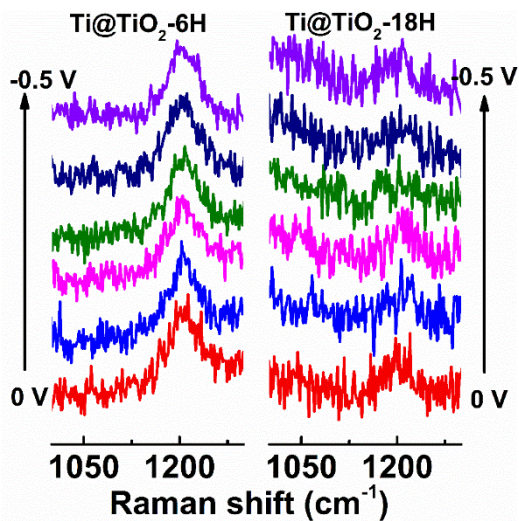


Figure S15. In situ Raman spectra of H adsorption on the Ti@TiO<sub>2</sub>-6H nanosheets in a 1.0 M KOH solution.

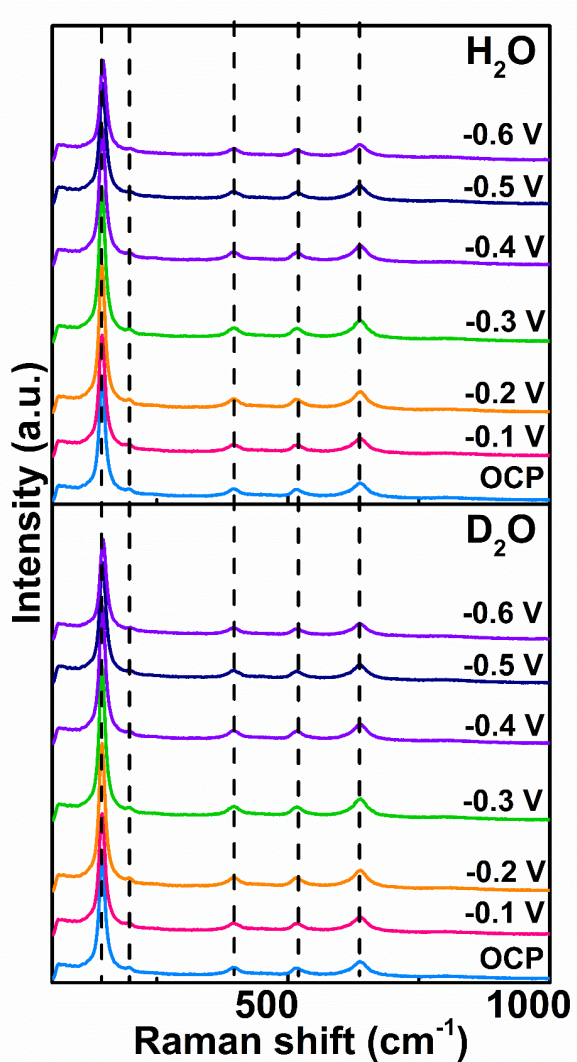


Figure S16. In situ Raman spectra of anatase Ti@TiO<sub>2</sub>-6H nanosheets in 1.0 M KOH or 1.0 M KOD solution below 1200 cm<sup>-1</sup>.

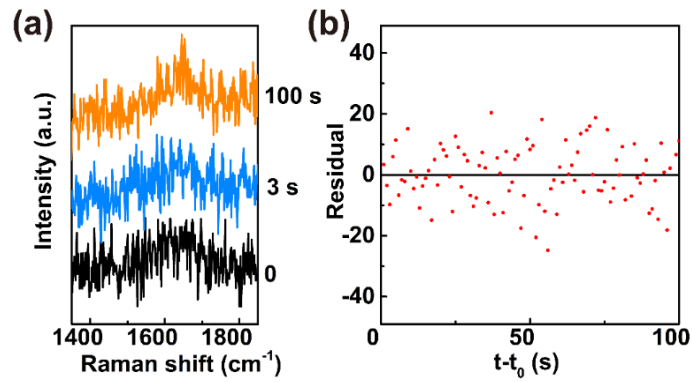


Figure S17. (a) Time-resolved Raman spectra of Ti@TiO<sub>2</sub>-6H nanosheets from 0 V to -0.5 V vs. RHE in a solution 0.5 M KOH (b) The fitting residual of HER of Ti@TiO<sub>2</sub>-6H in Figure 4c.

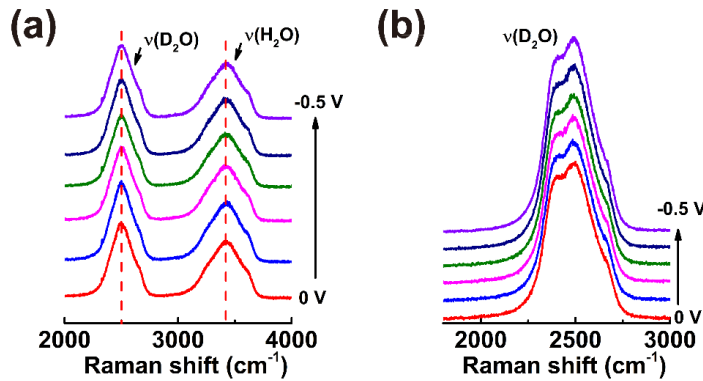


Figure S18. (a) The three peaks of interfacial water at  $\sim 3500 \text{ cm}^{-1}$  of Ti@TiO<sub>2</sub>-6H nanosheets from 0 V to -0.5 V vs. RHE in different solution: (a) 0.5 M KOH + 0.5 M KOD and (b) 1 M KOH.

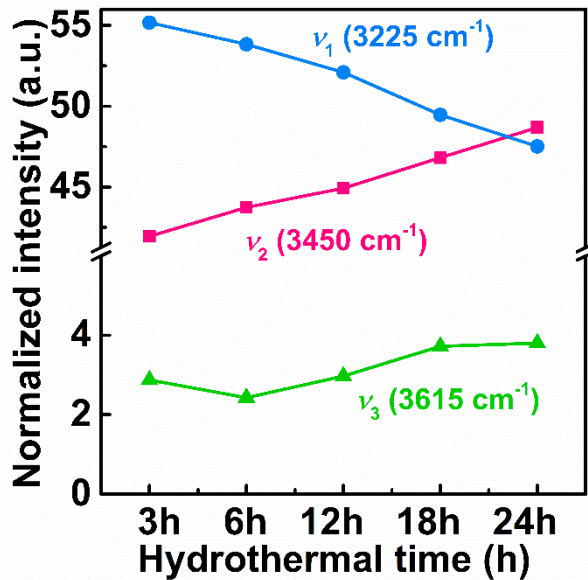


Figure S19. The normalized intensity of the three peaks of interfacial water on the surface of Ti@TiO<sub>2</sub> nanosheets with different hydrothermal time at -0.5 V vs. RHE in 1.0 M KOH solution.

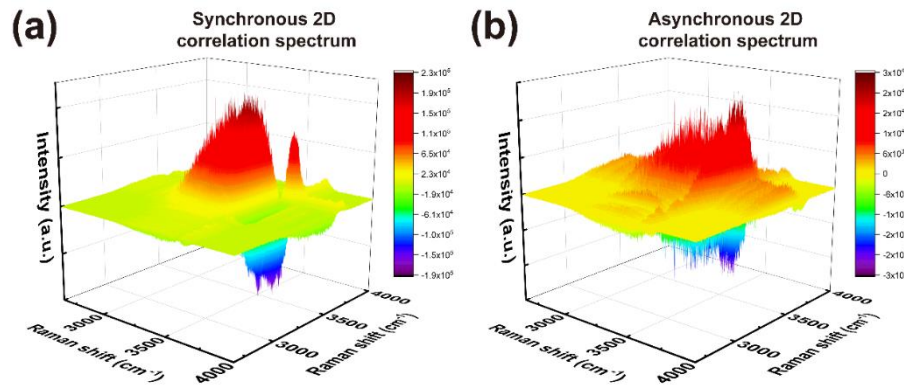


Figure S20. (a) Synchronous and (b) asynchronous 2D correlation Raman spectra of the interfacial water on the surface of Ti@TiO<sub>2</sub>-6H nanosheets from 0 V to -0.6 V vs. RHE.